

## **A manganese oxide nanozyme prevents oxidative damage of biomolecules without affecting the endogenous antioxidant system**

Namrata Singh,<sup>§,a,b,c</sup> Mohammed Azharuddin Savanur,<sup>§,b</sup> Shubhi Srivastava,<sup>b</sup> Patrick D'Silva,<sup>\*b</sup> Govindasamy Mugesh<sup>\*a</sup>

<sup>a</sup>Department of Inorganic and Physical Chemistry, Indian Institute of Science, Bangalore 560 012, India

<sup>b</sup>Department of Biochemistry, Indian Institute of Science, Bangalore 560012, India

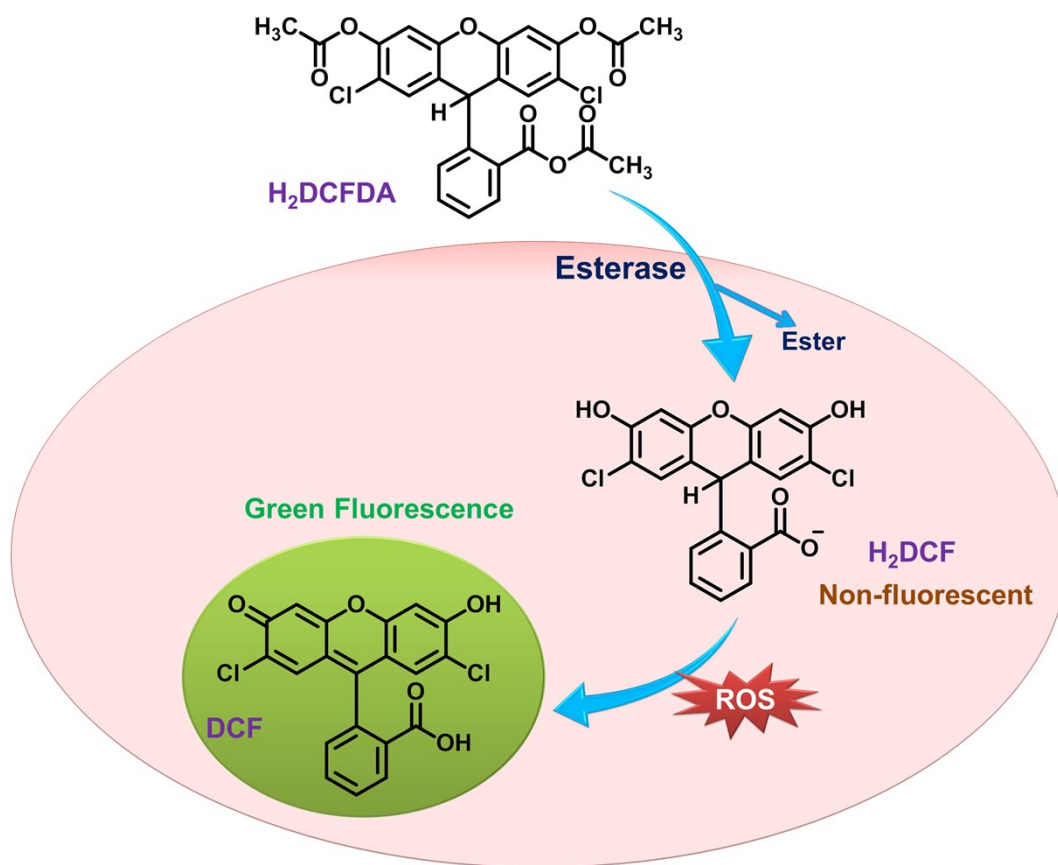
<sup>c</sup>Center for Nanoscience and Engineering, Indian Institute of Science, Bangalore 560012, India

<sup>§</sup>The authors contributed equally to this work.

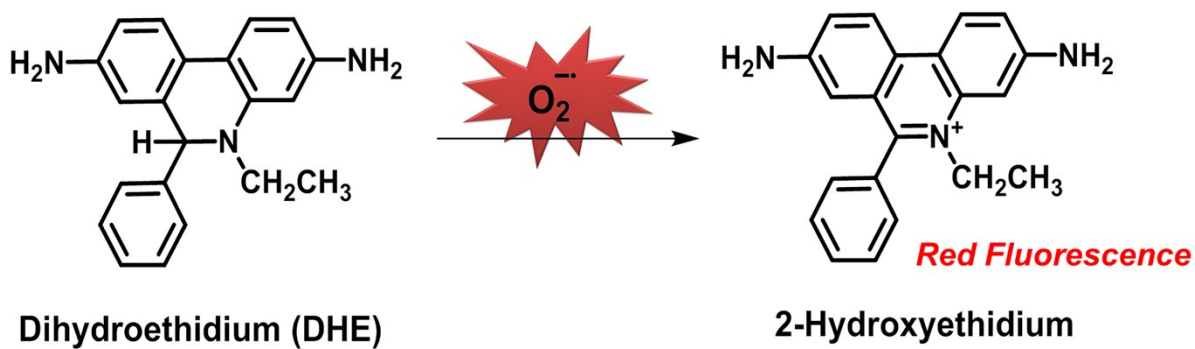
\*Corresponding authors

### **Table of Contents:**

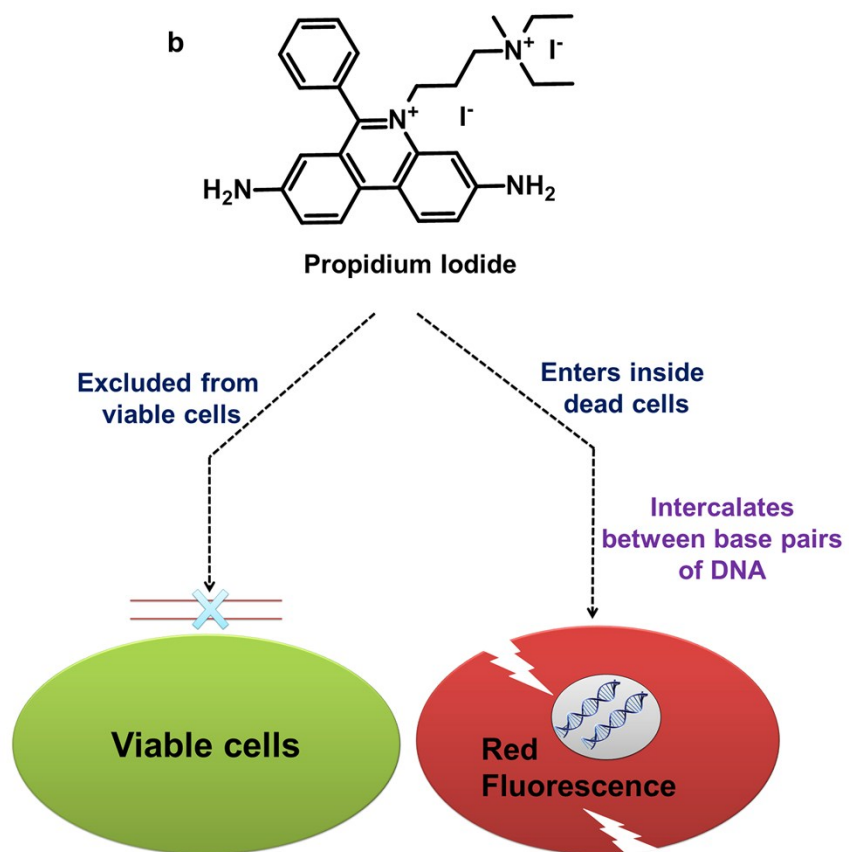
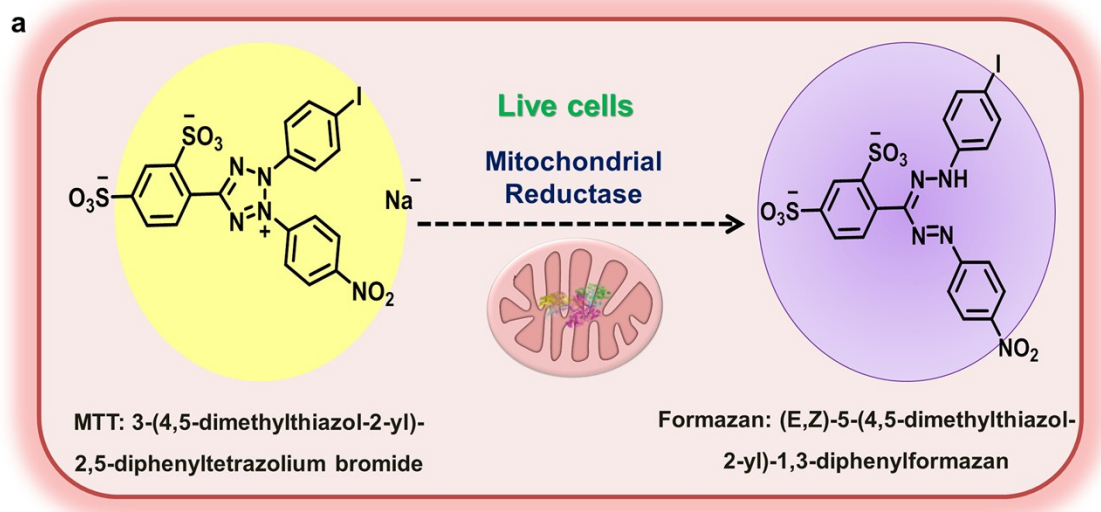
- **Scheme S1** - Scheme showing DCFDA action in cells.
- **Scheme S2** - Superoxide detection by DHE dye.
- **Scheme S3** - Assays utilized to determine cell viability. a) MTT assay and b) PI staining assay.
- **Scheme S4** - Inhibitors used in this study and their mode of action.
- **Scheme S5** - Protein carbonylation and its detection by DNPH.
- **Scheme S6** - Lipid peroxidation and its detection.
- **Figure S7-S12** - Characterization of precursor (Mo) and Mn<sub>3</sub>O<sub>4</sub> nanoparticles.
- **Figure S13** - EDX of cellular depressions.
- **Figure S14** - Effect of variable concentrations of Mp on cellular ROS levels and on viability of HEK293T cells.
- **Figure S15** - Effect of Mp on cellular ROS levels in SHSY-5Y cells.
- **Figure S16** - Effect of dose and incubation time of Mn<sub>3</sub>O<sub>4</sub> nanoparticles (Mp) on the viability of HEK293T cells.
- **Figure S17** - Antioxidant activity of Mp IN HEK293T cells
- **Figure S18** - Effect of Mn<sub>3</sub>O<sub>4</sub> nanoparticles on mitochondrial ROS.
- **Figure S19** - Quantification of protein carbonylation and DNA damage.



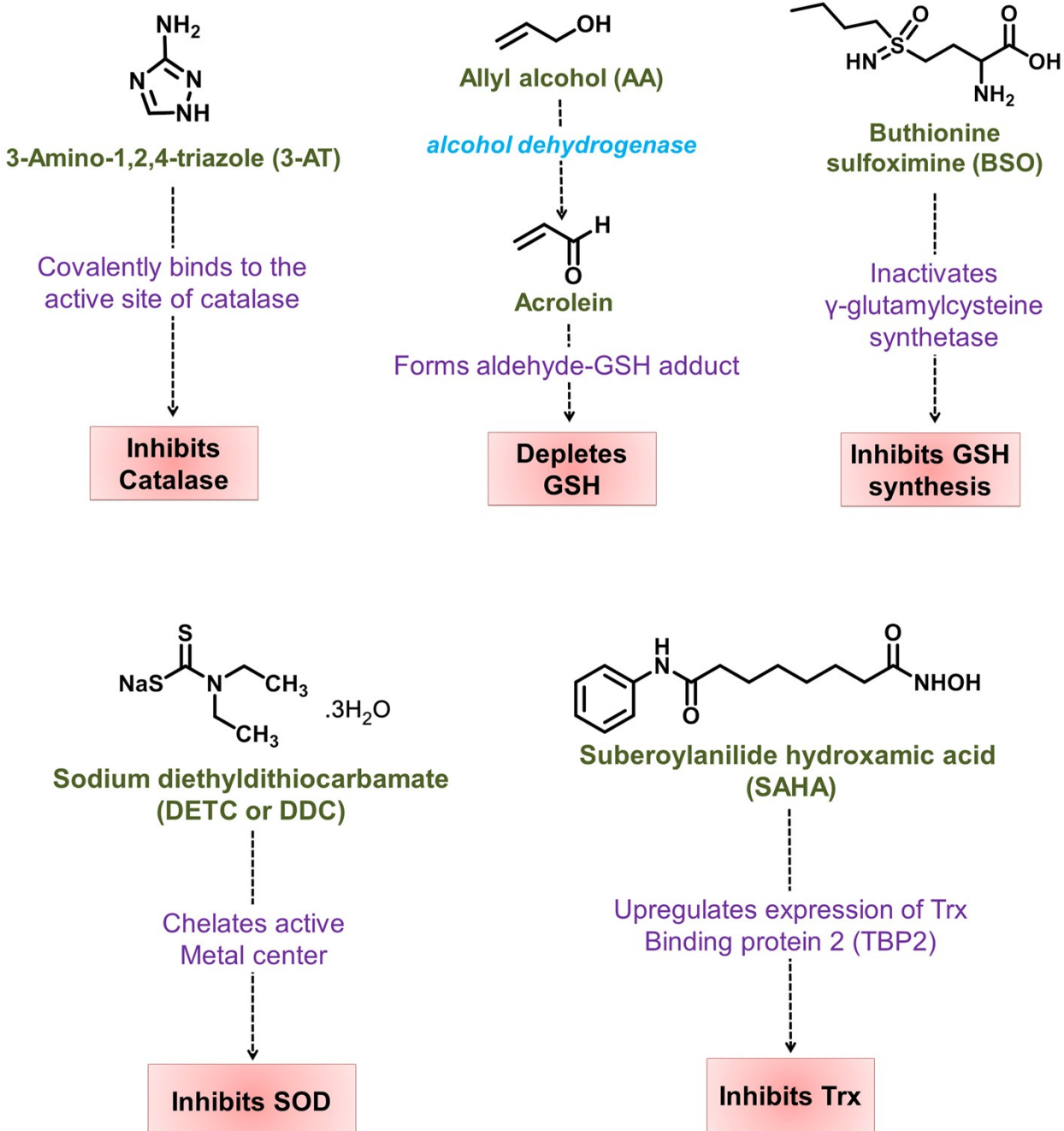
**Scheme S1.** ROS detection by DCFDA dye.



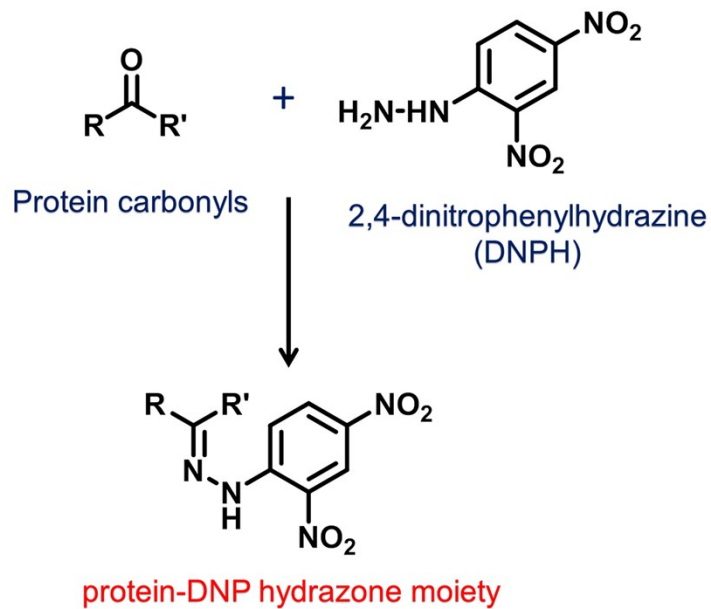
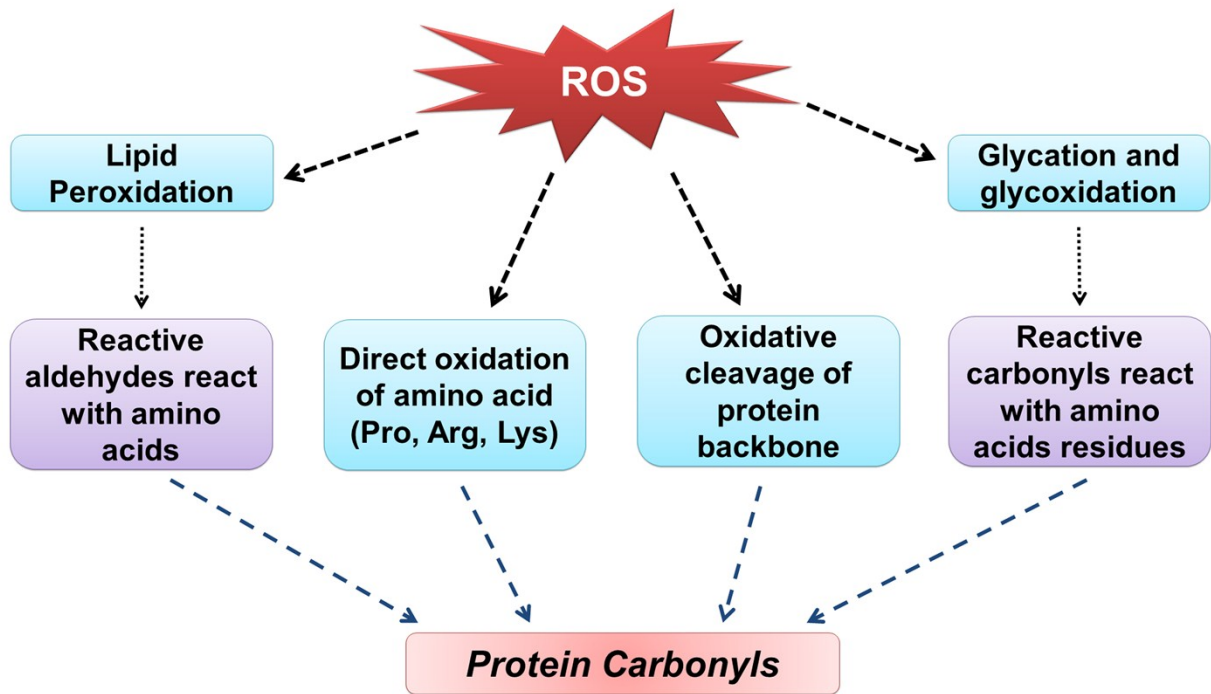
**Scheme S2.** Superoxide detection by DHE dye.



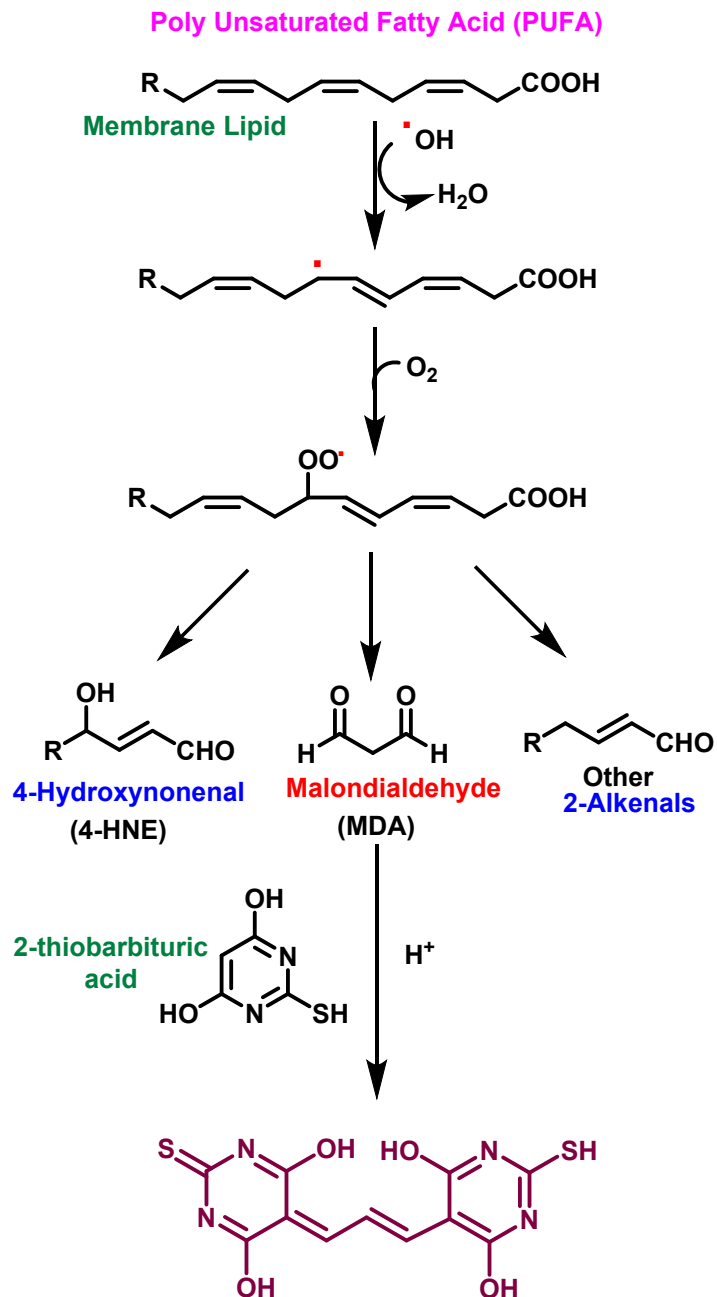
**Scheme S3.** Assays utilized to determine cell viability. a) MTT assay and b) PI staining assay.



**Scheme S4.** Inhibitors used in this study and their mode of action.



**Scheme S5.** Protein carbonylation and its detection by DNPH.



**Scheme S6.** Reactive aldehydes such as malondialdehyde (MDA), 4-hydroxy-2-nonenal (4-HNE) and other alkenals are generated as a result of reaction between ROS and lipid membranes. MDA reacts with 2-thiobarbituric acid to form a red product which can be detected colorimetrically at 532 nm.

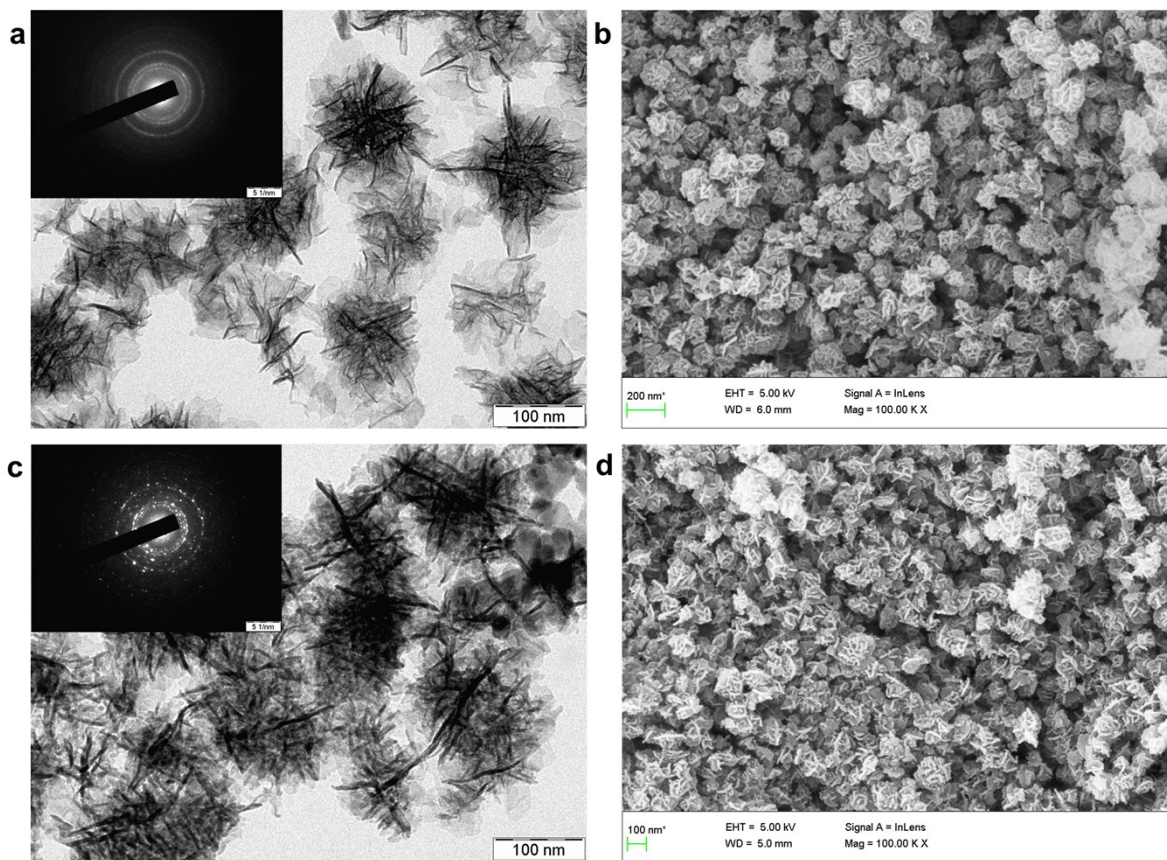


**Figure S7.** SEM and TEM micrographs of precursor particles a, b)  $\text{MnO}_2$  (Mo) showing monodisperse nanospheres. c, d)  $\text{Mn}_3\text{O}_4$  nanoparticles (Mp) obtained after calcination of precursor Mo particles at  $200\text{ }^\circ\text{C}$ . Inset showing the SAED pattern.

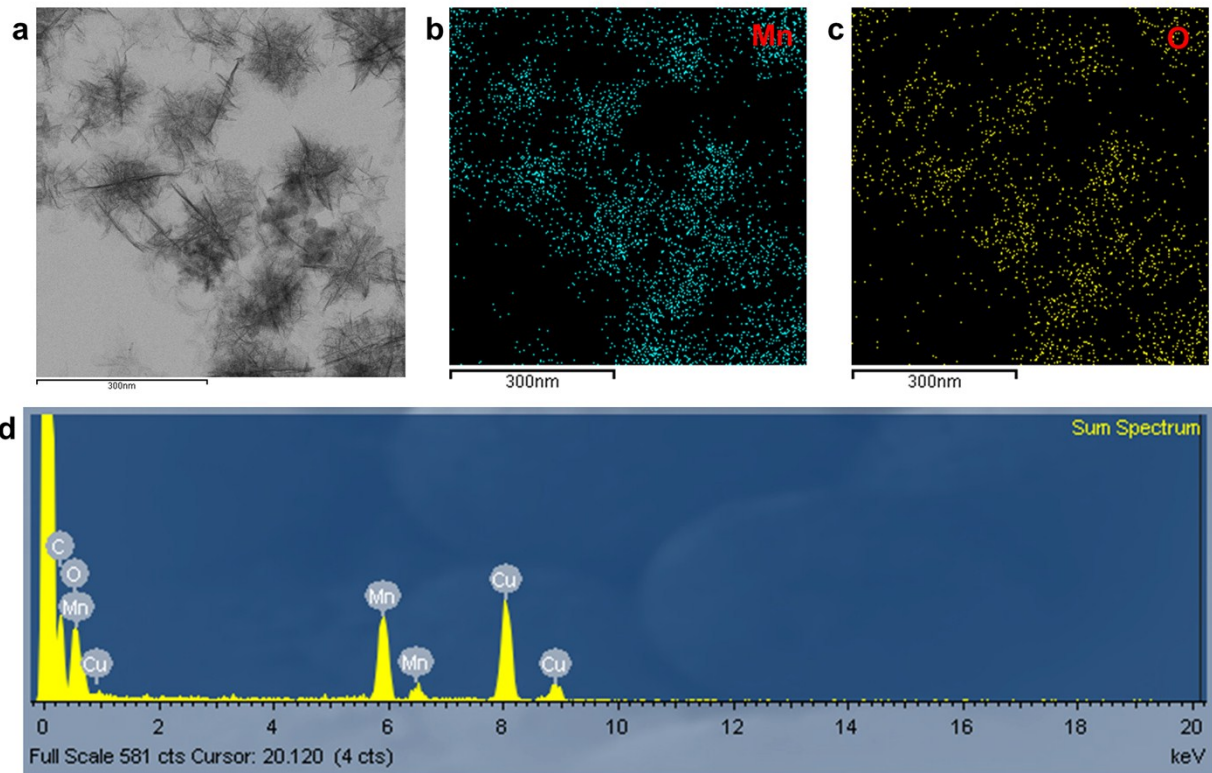


**Figure S8.** a-c) The X-ray mapping images showing elemental distributions of Mn and O in the precursor particles. d) Energy-dispersive X-ray spectra (EDX) of Mo showing the peaks of Mn and O. The presence of Cu and C peaks in the spectra is from the Cu-C grid used for drop-casting the sample.



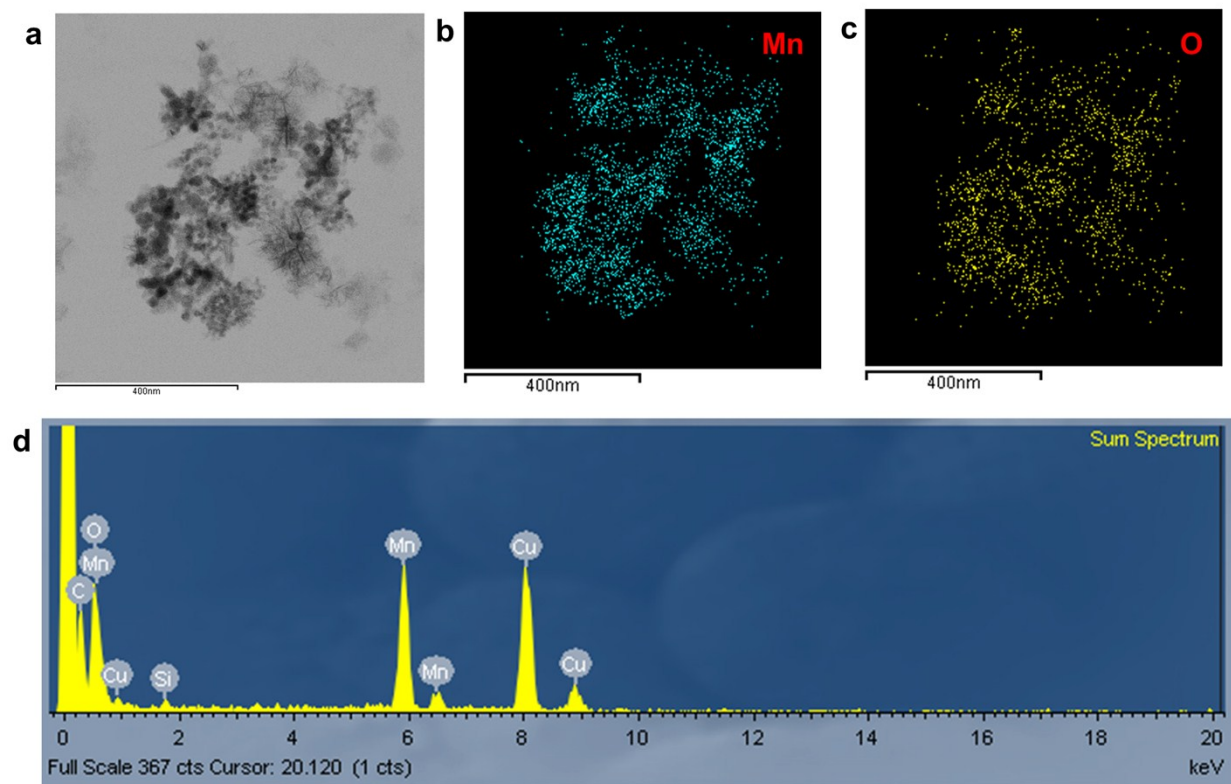


**Figure S9.** X-ray mapping images and EDX spectra of Mn<sub>3</sub>O<sub>4</sub> nanoparticles (Mp). a-c) The distribution of manganese (Mn) atom is indicated in blue color and the distribution of oxygen (O) atom is represented in yellow color. d) The EDX spectra confirm the presence of Mn and O in the sample.

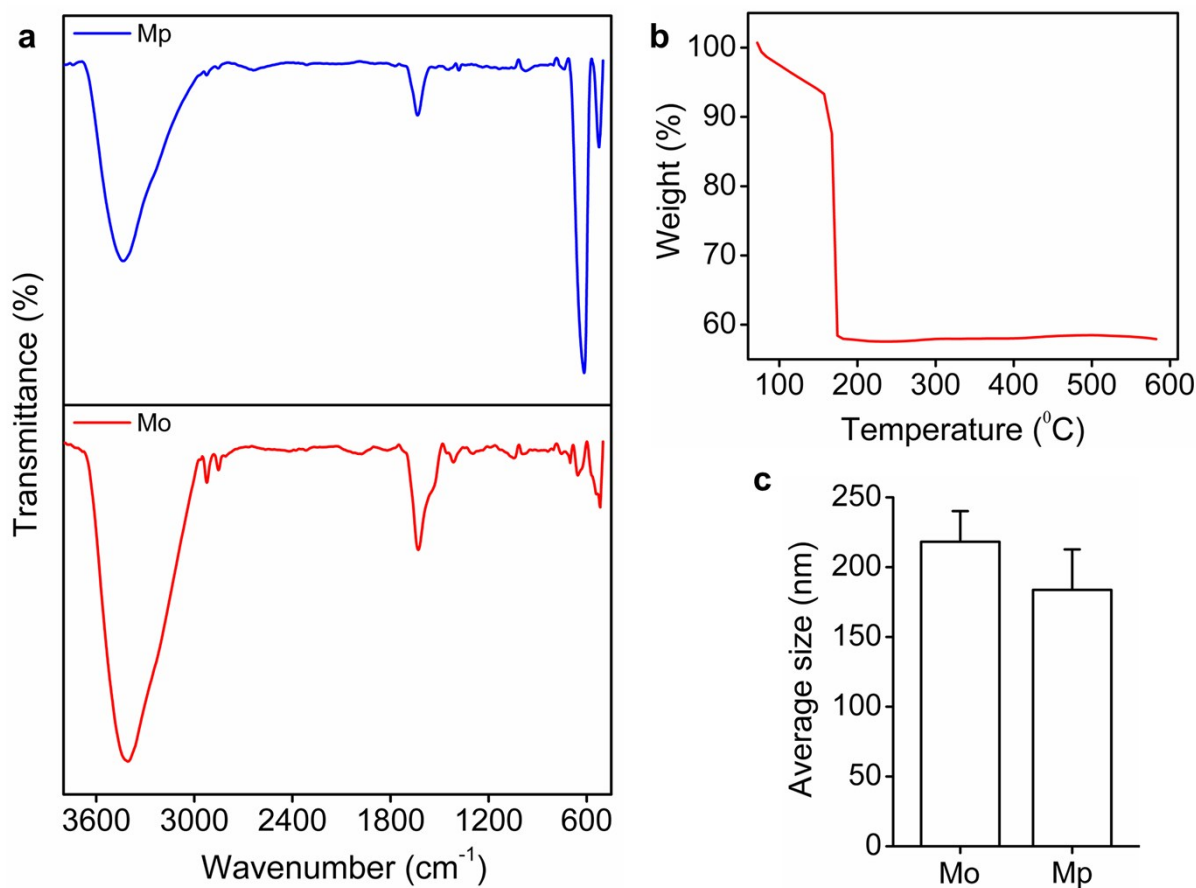


**Figure S10.** a) FTIR spectra of precursor particle (Mo, MnO<sub>2</sub>) and Mn<sub>3</sub>O<sub>4</sub> nanoparticles (Mp). The peak at 520 cm<sup>-1</sup> in the precursor sample can be assigned to layered MnO<sub>2</sub> (Red color plot) and the two prominent peaks at around 519 and 613 cm<sup>-1</sup> can be attributed to Mn<sub>3</sub>O<sub>4</sub> nanoparticles (Blue color plot). A broad peak at 3200-3600 cm<sup>-1</sup> and another peak at 1600 cm<sup>-1</sup> in both the spectra's corresponds to the stretching and bending vibration of the H<sub>2</sub>O and OH<sup>-</sup> in the lattice. The precursor sample showing peaks near 2800-3000 cm<sup>-1</sup> is assigned to the characteristic peaks of oleic acid, indicating the presence of oleic acid in the precursor sample which was absent in the calcined product, Mn<sub>3</sub>O<sub>4</sub>. b) TGA curve of precursor particles (Mo) indicating weight loss and phase change around 200 °C. c) Plot of average size of precursor particles (Mo) and Mn<sub>3</sub>O<sub>4</sub> nanoparticles (Mp).

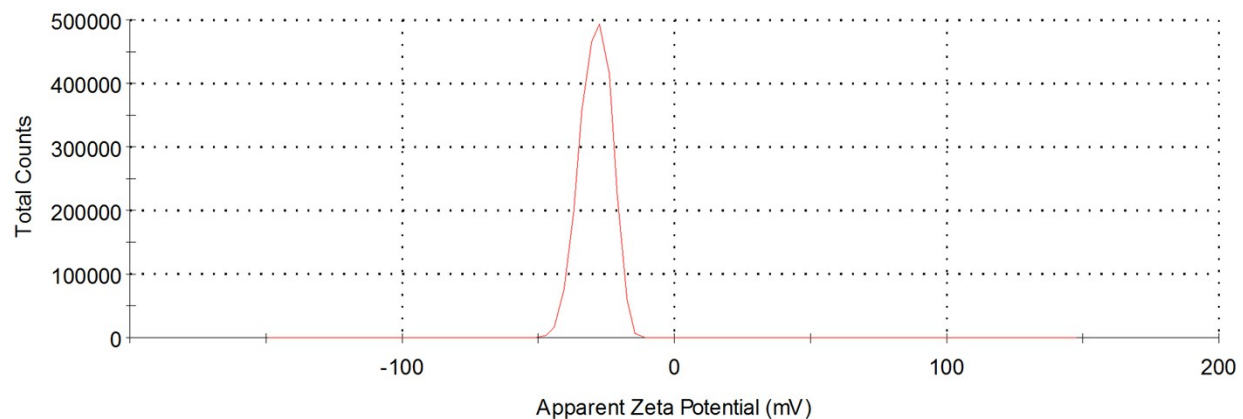


**Figure S11.** The zeta potential value of  $\text{Mn}_3\text{O}_4$  nanoparticles.

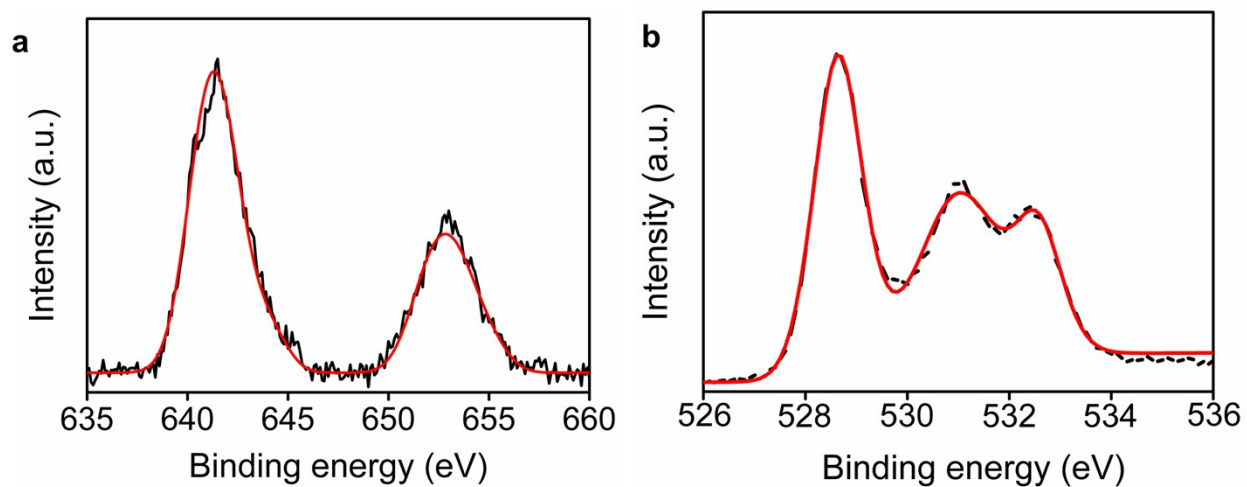


**Figure S12.** a-b) The XPS (X-ray photoelectron spectroscopy) spectra of Mn and O in  $\text{Mn}_3\text{O}_4$  nanoparticles, respectively.

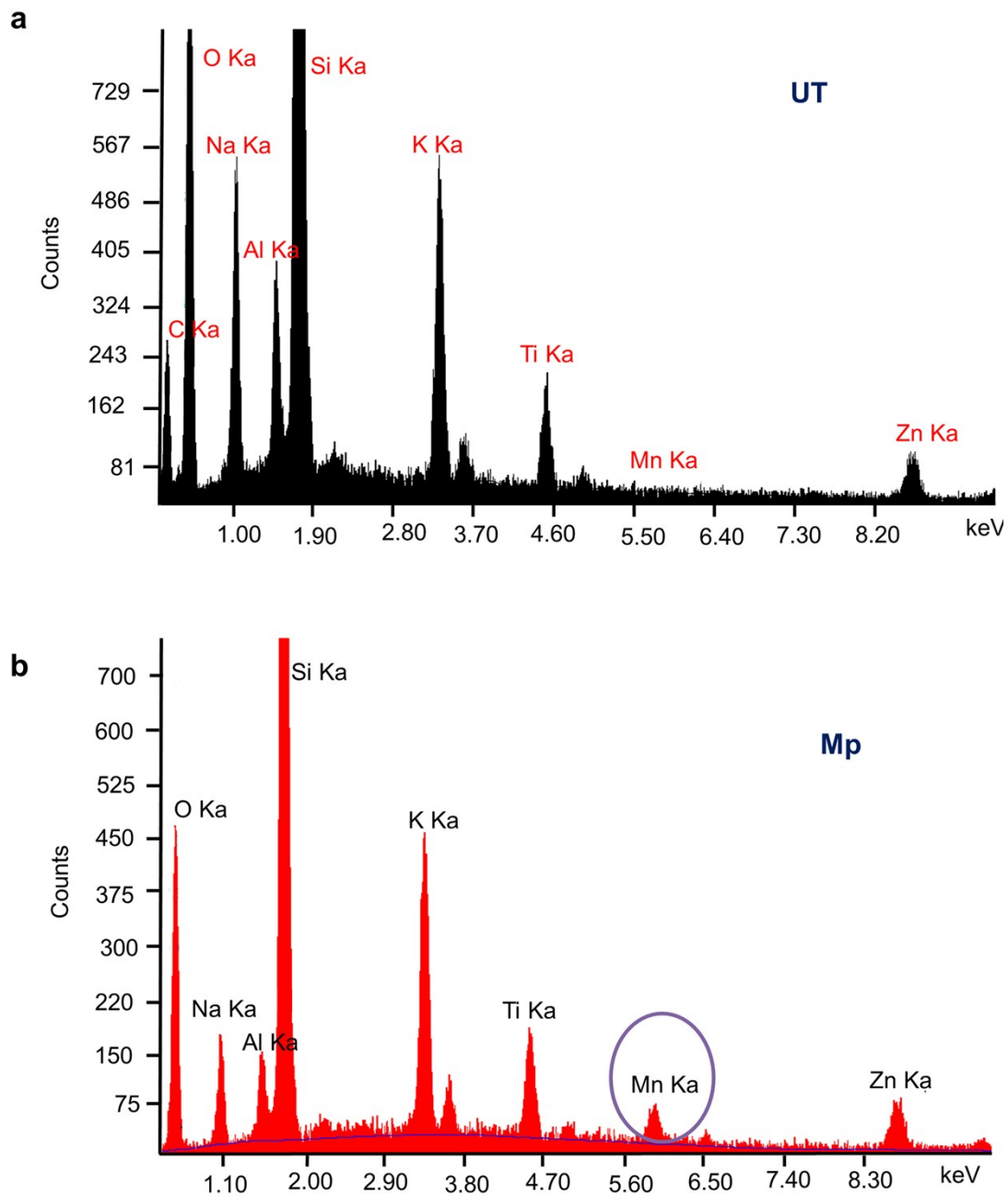


**Figure S13.** a-b) The EDX (Energy-dispersive X-ray spectroscopy) spectra of cellular depressions without gold coating the samples.

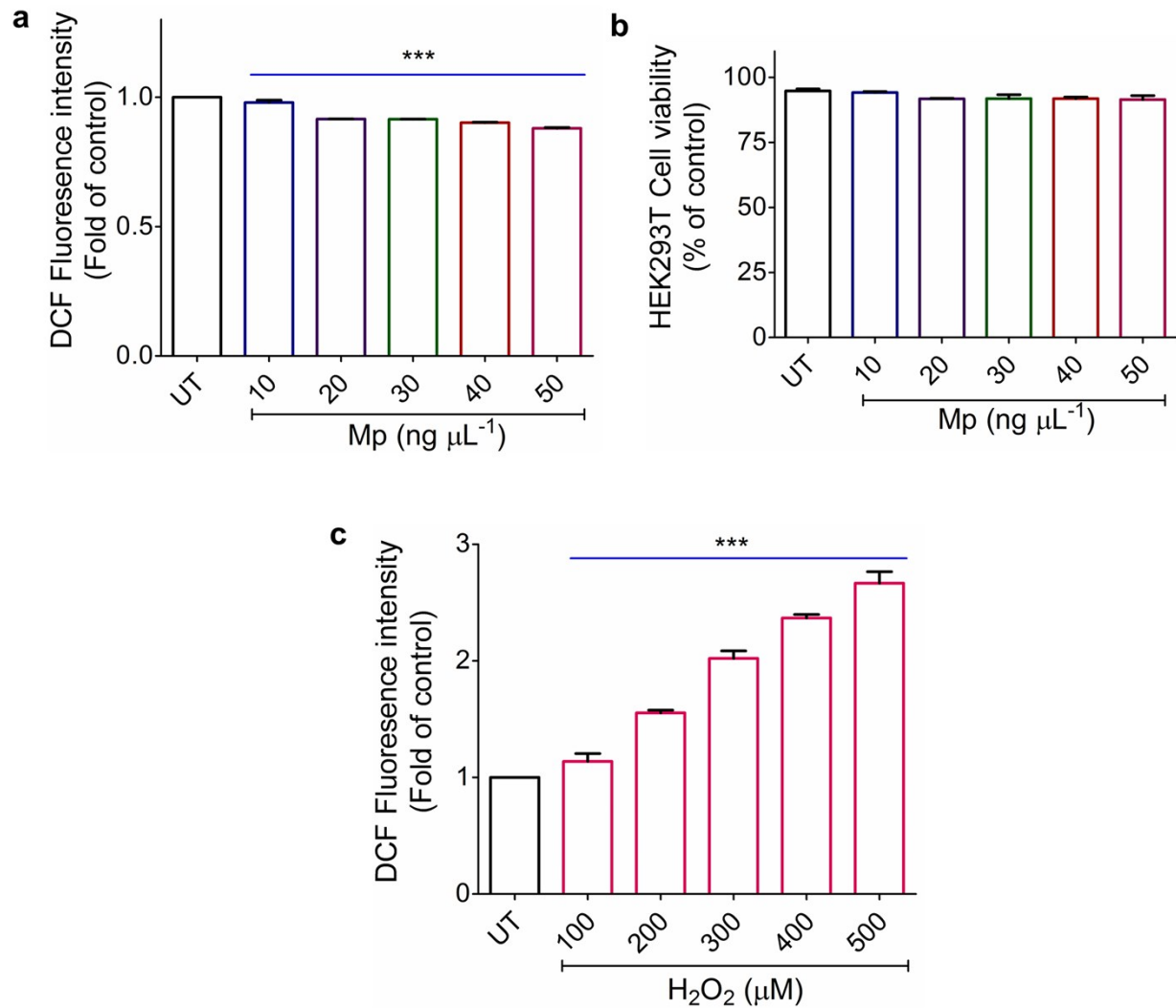


**Figure S14.** a, b) Effect of variable concentrations of Mp on cellular ROS levels and on the viability of HEK293T cells. Cells were exposed to increasing concentration of Mp for 15 min followed by measurement of cellular ROS level and viability in flow cytometer using DCFDA-H2 and PI fluorescent dyes respectively. c) Effect of increasing concentration of H<sub>2</sub>O<sub>2</sub> on cellular ROS levels was analysed by flow cytometry using DCFDA-H2. Data represented as mean  $\pm$  s.e.m., n=3, \*\*\*P (t-test) < 0.0001.

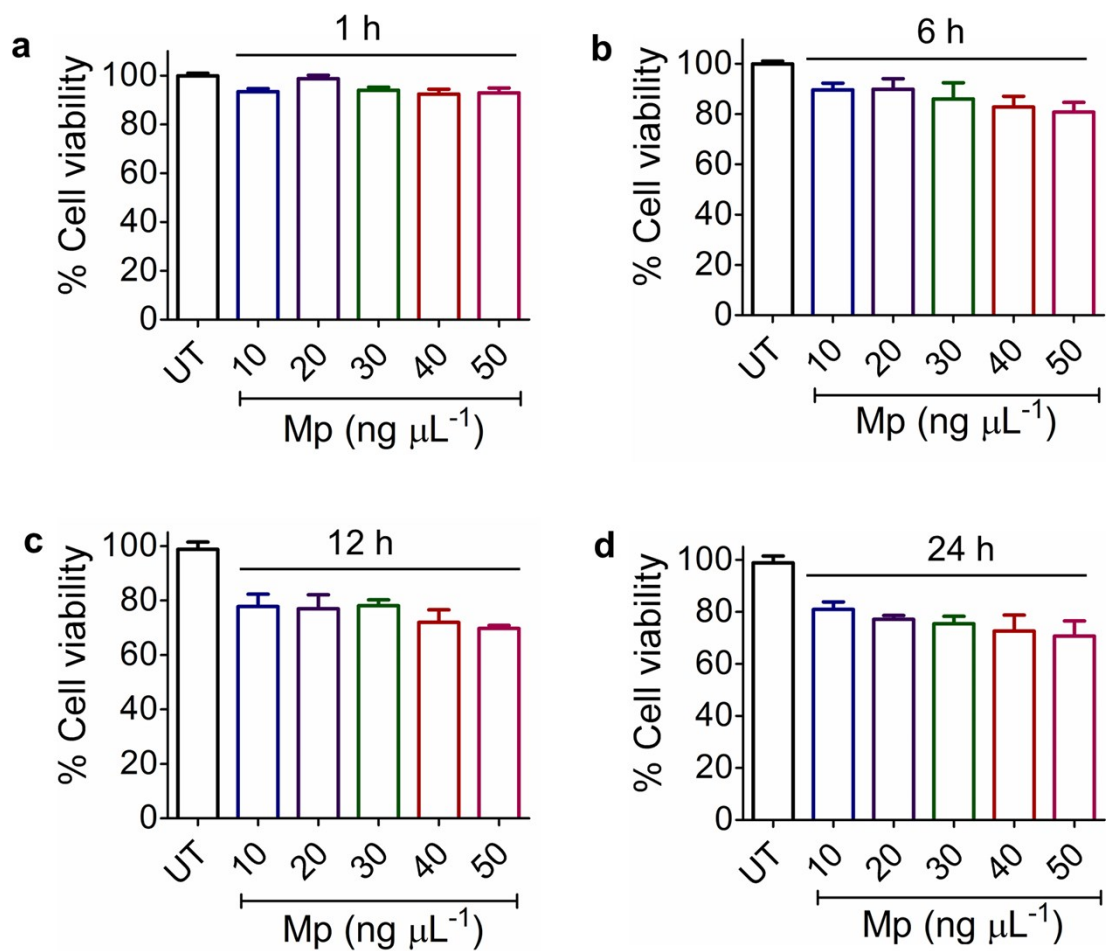


**Figure S15.** Effect of dose of  $Mn_3O_4$  nanoparticles (Mn) and incubation time on the viability of HEK293T cells. Cells were exposed to variable concentrations of Mn and were incubated for different time intervals a) 1h, b) 6h, c) 12h and d) 24h followed by cell viability measurement using MTT assay. Data represented as mean  $\pm$  s.e.m.,  $n=3$ , \*\*\*P (t-test)  $< 0.0001$ .

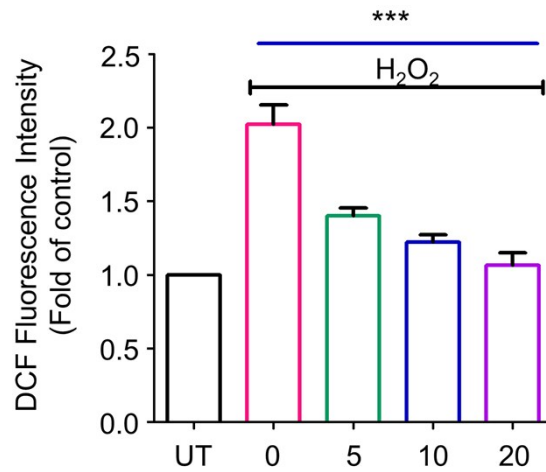


**Figure S16.** ROS scavenging activity of Mp in neuroblastoma cells (SHSY-5Y) was evaluated by pre-treating the cells with Mp followed by exposure to H<sub>2</sub>O<sub>2</sub> and determined by flow cytometry using DCFDA-H<sub>2</sub> dye. Data is represented as fold mean fluorescence intensity over untreated cells. Bars denote mean  $\pm$  s.e.m., n=3, \*\*\*P < 0.0001.

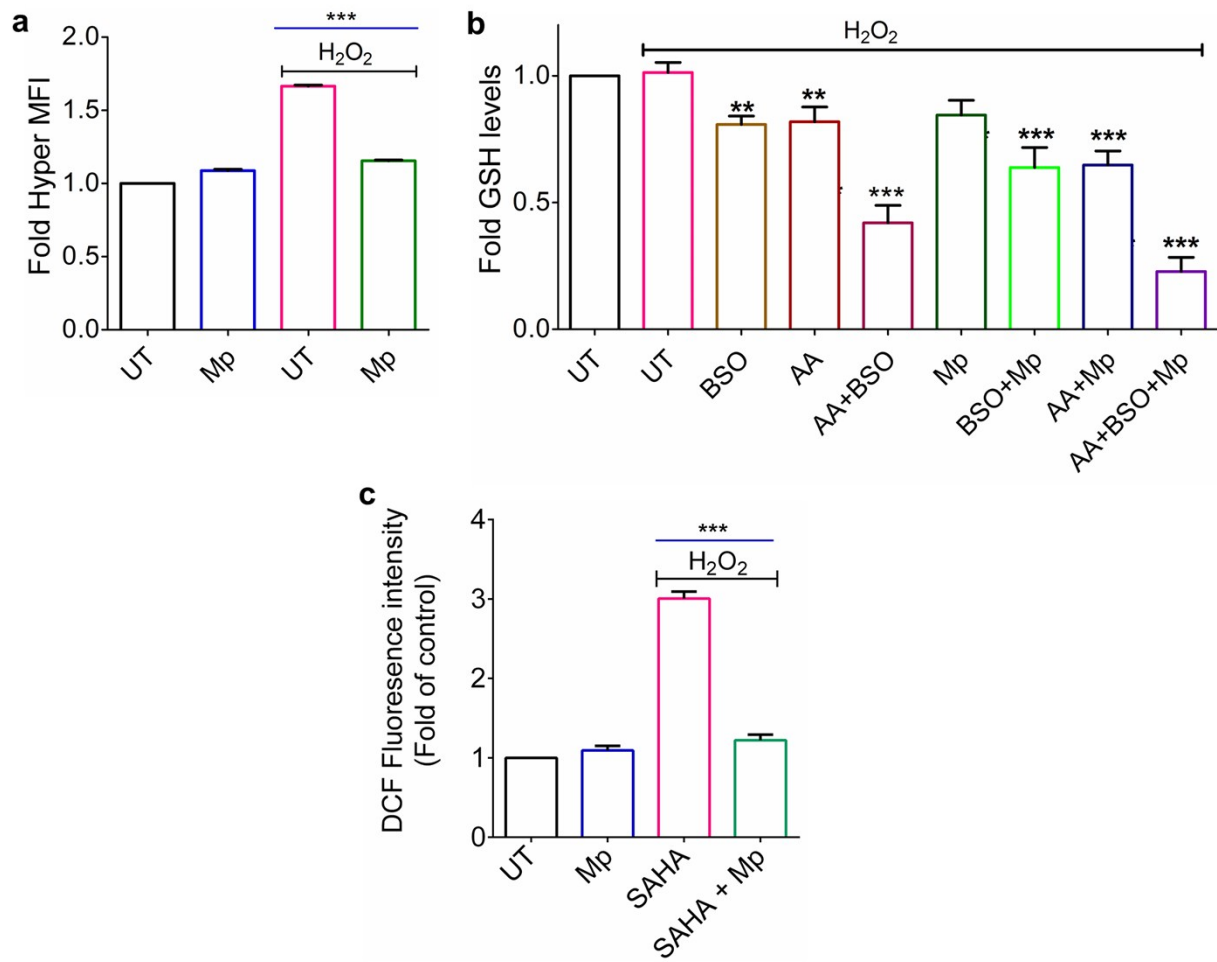


**Figure S17.** a) H<sub>2</sub>O<sub>2</sub> scavenging ability of Mp was determined by using genetically encoded fluorescent probe HyPer specific to H<sub>2</sub>O<sub>2</sub>. HEK293T cells were transfected with the plasmid encoding HyPer for measurement of ROS using Lipofectamine 2000. Post 48h incubation, the cells were treated with similar protocol followed for ROS measurement and the relative HyPer fluorescence intensity was analysed spectrophotometrically. b) The cellular GSH level was quantified in HEK293T cells treated with Mp and GSH inhibitors (BSO and AA) using GSH-Glo kit (Promega). c) HEK293T cells were pre-incubated with SAHA (7.5 μM) for 5 h prior to Mp and H<sub>2</sub>O<sub>2</sub> treatment. The cellular ROS levels were analysed using DCFDA-H2 by flow cytometry. Bars denote mean ± s.e.m., n=3, \*\*\*P (t-test) < 0.0001.



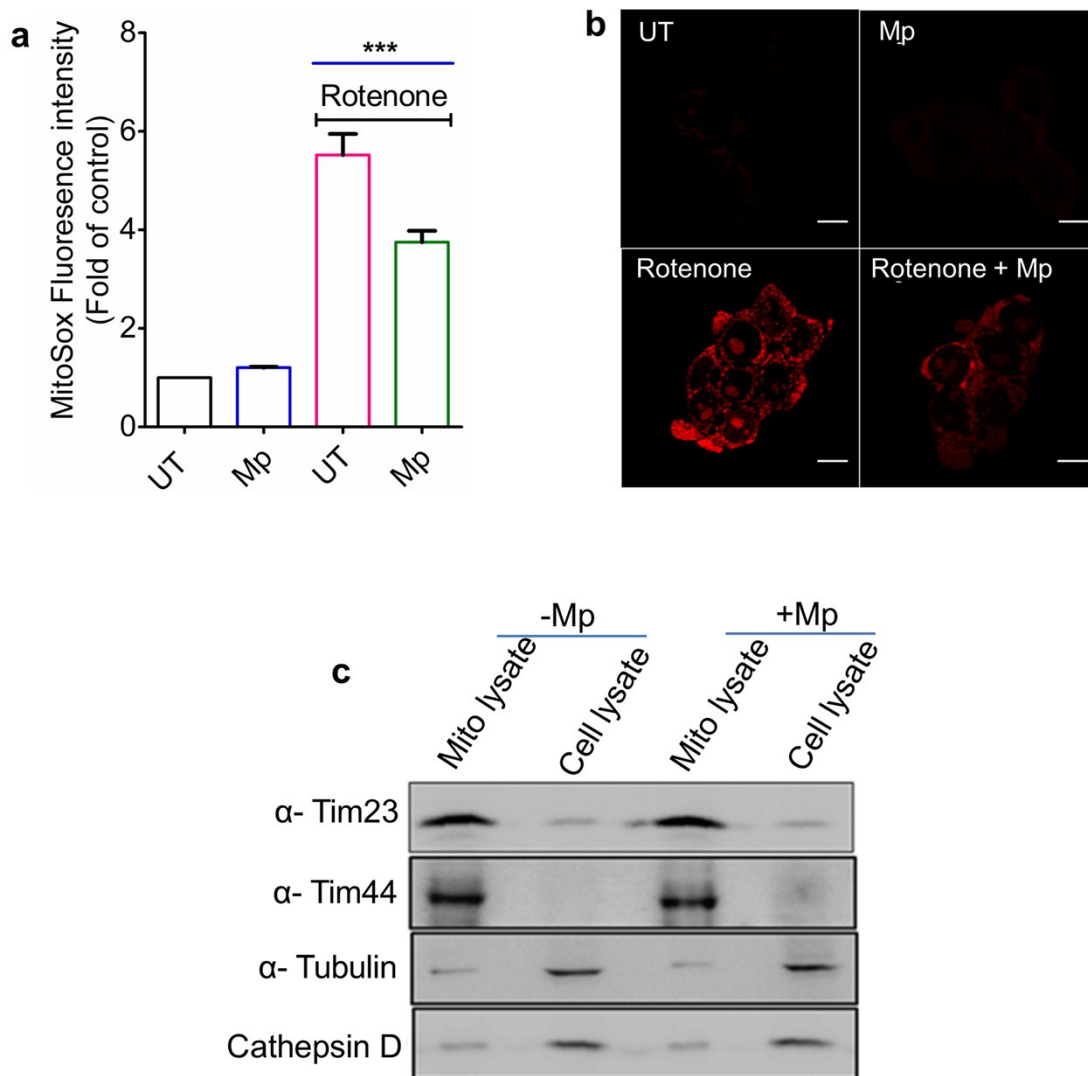


**Figure S18.** a, b) The ability of Mp to scavenge superoxide generated in mitochondria was evaluated by mitochondrial superoxide specific dye MitoSox. Cells were pre-treated with Mp followed by Rotenone treatment, and the generation of superoxide radicals was analyzed by flow cytometry and fluorescence microscopy. Bars denote mean  $\pm$  s.e.m.,  $n=3$ ,  $***P$  (t-test)  $< 0.0001$ . c) Western blots indicating purity of mitochondrial fraction. Blots were probed with anti-Tim23 and Tim44 antibodies for mitochondrial control, anti-Tubulin and Cathepsin D for cytosolic control.

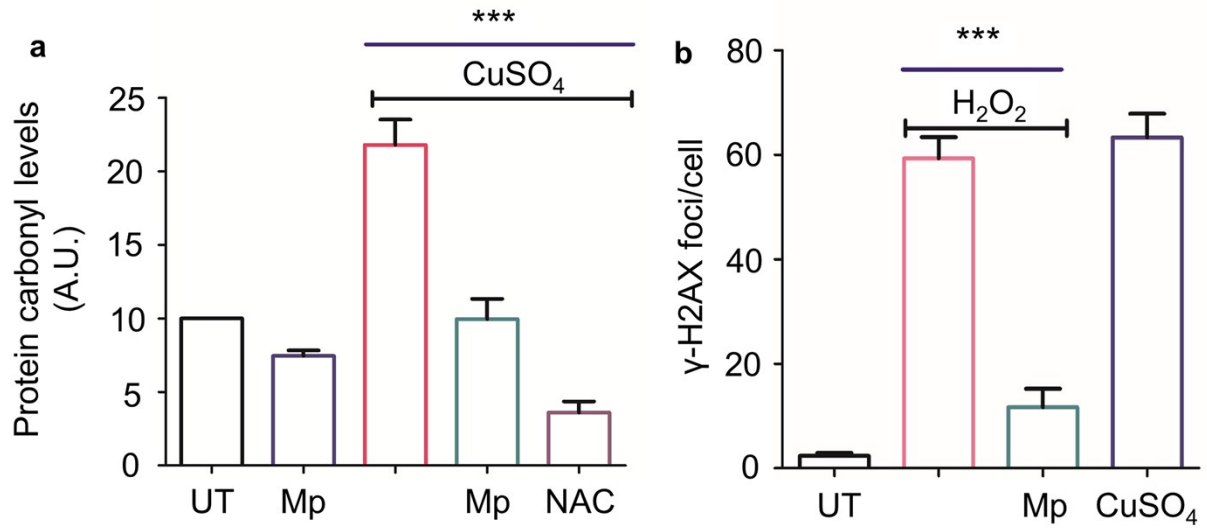


**Figure S19.** Quantification of protein carbonylation and DNA damage in HEK293T cells. a) The bar graph represents densitometry analysis of total protein carbonyl levels relative to untreated control and represented as mean  $\pm$  s.e.m, n=3, \*\*\*P< 0.0001. b) The graph shows relative number of  $\gamma$ -H2AX foci formed as compared to untreated control. Data is presented as mean  $\pm$  s.e.m, n=3, \*\*\*P<0.0001.